Monthly Progress Report P-B1980-6

HERO SUPPORTING STUDIES

by

Norman P. Faunce
Paul F. Mohrbach

December 1 to December 31, 1962

Prepared for

U.S. NAVAL WEAPONS LABORATORY
Dahlgren, Virginia

Contract No. N178-8102

THE FRANKLIN INSTITUTE
LABORATORIES FOR RESEARCH AND DEVELOPMENT
PHILADELPHIA PENNSYLVANIA

THE FRANKLIN INSTITUTE • *Laboratories for Research and Development*

(9) Monthly Progress Report

(4) See cover
(5) 501 500

(14) Rept. no. P-B1980-6

(6) HERO SUPPORTING STUDIES

(7) NA
(8) GU
(11) 31 Dec 62
(12) 27p.
(13) NA
(16) NA
(17) NA
(18) NA
(19) NA
(21) NA

(10) by

Norman P. Faunce and
Paul F. Mohrbach

(1) December to (31) December, 1962

Prepared for

U.S. Naval Weapons Laboratory
Dahlgren, Virginia

(15) Contract ~~No.~~ N178-8102

P-B1980-6

ABSTRACT

Two prototype models of low band pass transformers being developed for Naval Weapons Laboratory, Dahlgren, were evaluated. Each was found to provide more than 40 db loss from 20 Kc to 1 Mc, and at 1 and 10 Gc. Temperature rise with 10 watts input was determined to be less than 100°C in 30 minutes, well within specifications.

A theoretical development is given which shows the order of magnitude of changes in alternate maximum and minimum voltages on a low loss transmission line having a high VSWR. It was found that in transmission lines normally assumed lossless the change in successive voltage minima may be as high as 7%; for line that might be thought "low loss", the change could be considerably greater.

Voltage min-max power measurements $\left(P = \frac{V_{min} V_{max}}{Z_o} \right)$ in a waveguide are discussed. So as to avoid the Z_o concept in waveguide, power is determined by the expression $P = k \sqrt{D_{max} D_{min}}$ where D_{max} and D_{min} are voltage probe indications and k is an experimentally determined constant. Details of the method are given.

SUMMARY

Two prototype low band pass transformers (LBT's) developed by Weston Instruments were examined to find the terminated power loss, at low frequency and low power. With a one-ohm termination both gave greater than 40 db power loss in the 20 Kc to 1 Mc frequency range. The losses at 1 and 10 Gc are determined, and appear to be greater than 40 db. At these two higher frequencies, 10 watts of power were applied, and the temperature rise over a 30 minute interval was noted. Temperatures do not exceed 100°C for one unit, and 80°C for the other. From these data, unit number 58A appears more desirable. Power loss at 30 and 250 Mc are to be determined, and if input power can be raised to 5 or 10 watts we shall determine the temperature rise as well. On the basis of these data Weston will freeze their design, and prepare to develop final production models. These should be available for tests in early March at the latest.

A theoretical development was initiated to substantiate the large losses indicated for a supposedly lossless line by the results obtained with the voltage min-max method of power measurement. This analysis supported the experimental results and once more indicated that low loss line can become quite lossy when large standing waves occur on it.

In preparation for a high frequency evaluation of the protected MARK 7 MOD 0 ignition element we have investigated the voltage min-max power measuring technique adapted to waveguide. Because of the uncertainty of the concept of characteristic impedance in waveguide systems the defining equation was modified to eliminate this parameter, resulting in the expression.

$$P_n = k \sqrt{D_{max} D_{min}}$$

where D_{max} and D_{min} are related to V_{max} and V_{min}, and k is an experimentally determined constant.

Detailed procedures for a precision firing test are developed. It is first necessary to calibrate the slotted line probe. The probe is then used to measure a low level power supplied to a live item, and the power compared to the total power delivered to the system. This comparison results in a system efficiency factor which, when applied to actual firing power levels gives the power to the base of the device under test. The distinctive feature of this procedure, compared to earlier work, is that a source of small output power is used in place of the actual source used in the firing test. It is believed that this yields better accuracy.

Extension of this technique for pulse firing tests is under consideration. Some work is planned to resolve the many uncertain factors that appear to limit the feasibility of this approach. Some effort must be directed toward this problem before we can perform the stated pulse firings of the MARK 7 elements. Improvements to the technique for CW work may enhance the chances for successful pulse tests.

LIST OF FIGURES

1. EVALUATION OF PROTOTYPE LOW BAND-PASS TRANSFORMERS

Under contract with the Naval Weapons Laboratory, the Weston Instrument Division of Daystrom Corporation is developing a low band pass transformer (LBT), to by-pass low frequency currents and impede the flow of high frequency energy; 40 db or greater loss is required at 100 Kc and beyond. Furthermore, the unit must have the ability to dissipate 10 watts of power in the stop band.

Weston's testing capability is limited to frequencies below 100 Kc. They have therefore requested Franklin Institute to evaluate their transformers from this point to a maximum of 10 Gc. Accordingly two prototype models were delivered for tests to determine which should be chosen as a final design. The essential difference, according to manufacturer's information, was that one had coils wound with asbestos insulated wire, the other uses a standard magnet wire.

The prototypes were delivered without connectors, the choice of approved couplings being still unsettled. Our test facility is designed around extensive use of coaxial transmission systems; these LBT's are of shielded twin-lead configuration. We were asked to evaluate the loss in accordance with the design use. Accordingly, General Radio connectors were mounted as indicated in Figure 1-1. This alteration distorts the "balanced-to-ground" feature typical to shielded twin lead components and should thereby degrade the loss characteristic of the item. Consequently if the item shows 40 db in this configuration, it should provide at least this amount when properly deployed.

We were asked to determine the power loss ratio while the transformers were terminated in a one-ohm load. Data was to be collected for several frequencies within 0.1 to 10,000 Mc. In addition we were to determine the temperature rise of the primary coil winding (and, if convenient, the secondary) with 10 watts of power applied. Temperature rise was to be determined at two or more frequencies.

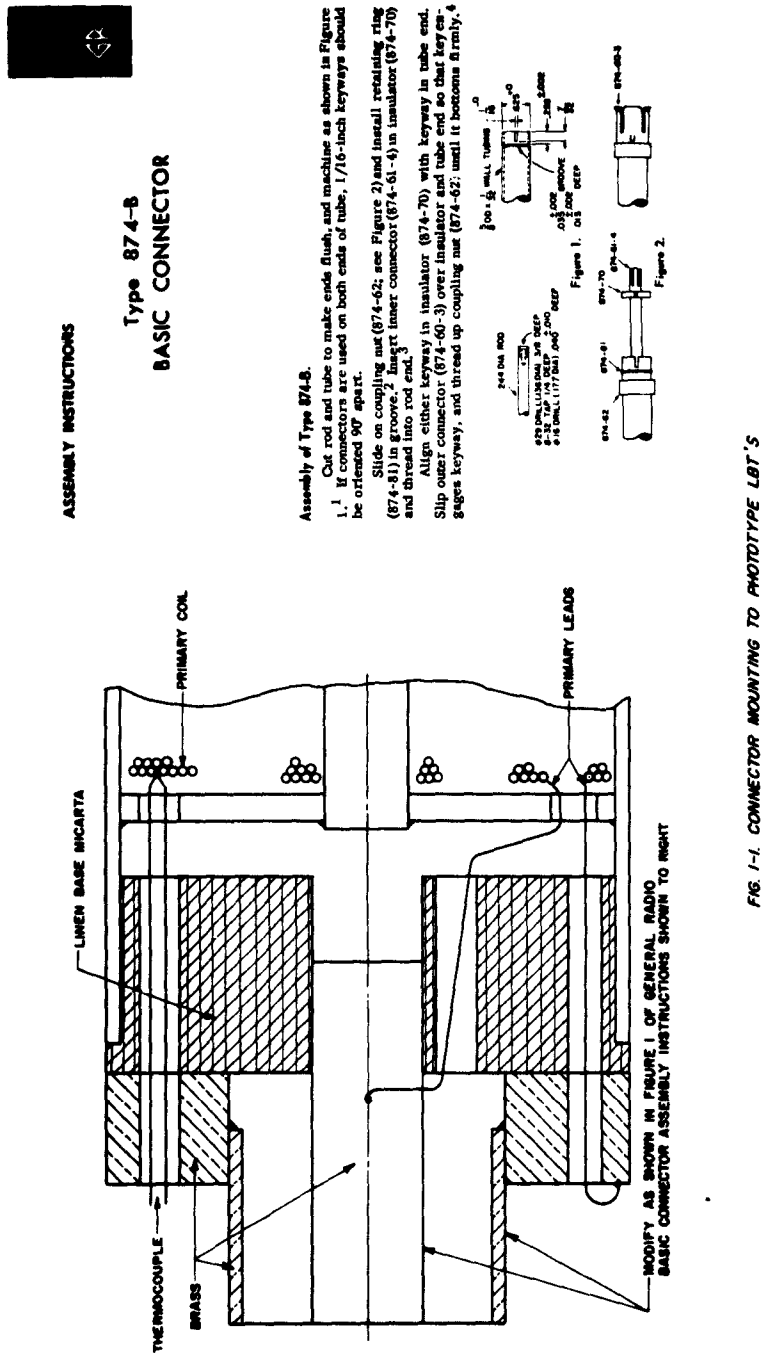

FIG. 1-1. CONNECTOR MOUNTING TO PHOTOTYPE LBT'S

So far, we have determined the power loss at 20, 100, 250, 500, 800 and 1000 Kc with low power excitation, and have estimated it to be greater than 40 db at 1000 and 10,000 Mc. We have determined the temperature rise, as well, at these latter frequencies.

Power loss measurements are summarized in Table 1-1 and are shown plotted in Figure 1-2.

Table 1

LOW POWER INPUT, POWER LOSS FOR PROTOTYPE LBT's

Frequency (Mc)	#57 P_{in} (watts)	#57 P_L (μ watts)	#57 TPL (db)	#58A P_{in} (watts)	#58A P_L (μ watts)	#58A TPL (db)
0.020	0.338	0.45	58.8	0.306	11.25	44.3
0.100	0.049	0.18	53.9	0.038	0.198	52.9
	(0.179)	(0.66)	(54.3)	-	-	-
0.250	0.018	0.003	68.1	0.165	0.011	71.6
0.500	0.021	0.003	68.8	0.086	0.001	78.3
	(5.781)	(0.125)	(76.7)	-	-	-
0.780	0.032	0.001	74.0	-	-	-
0.800	-	-	-	0.036	0.002	73.0
1.000	0.018	0.08	53.6	0.017	0.002	69.0

NOTE: $TPL\left(= 10 \log \frac{P_{in}}{P_L}\right)$ given is for P_{in}/P_L before P_L is rounded off to the three places shown.

The data indicated by arrows in the Figure were determined at a power level above which evidence of distortion was observed. Because of the technique used, distortion precludes a reliable determination. It had been agreed in discussing these tests with a Weston representative that it was of paramount interest to demonstrate that these units would provide

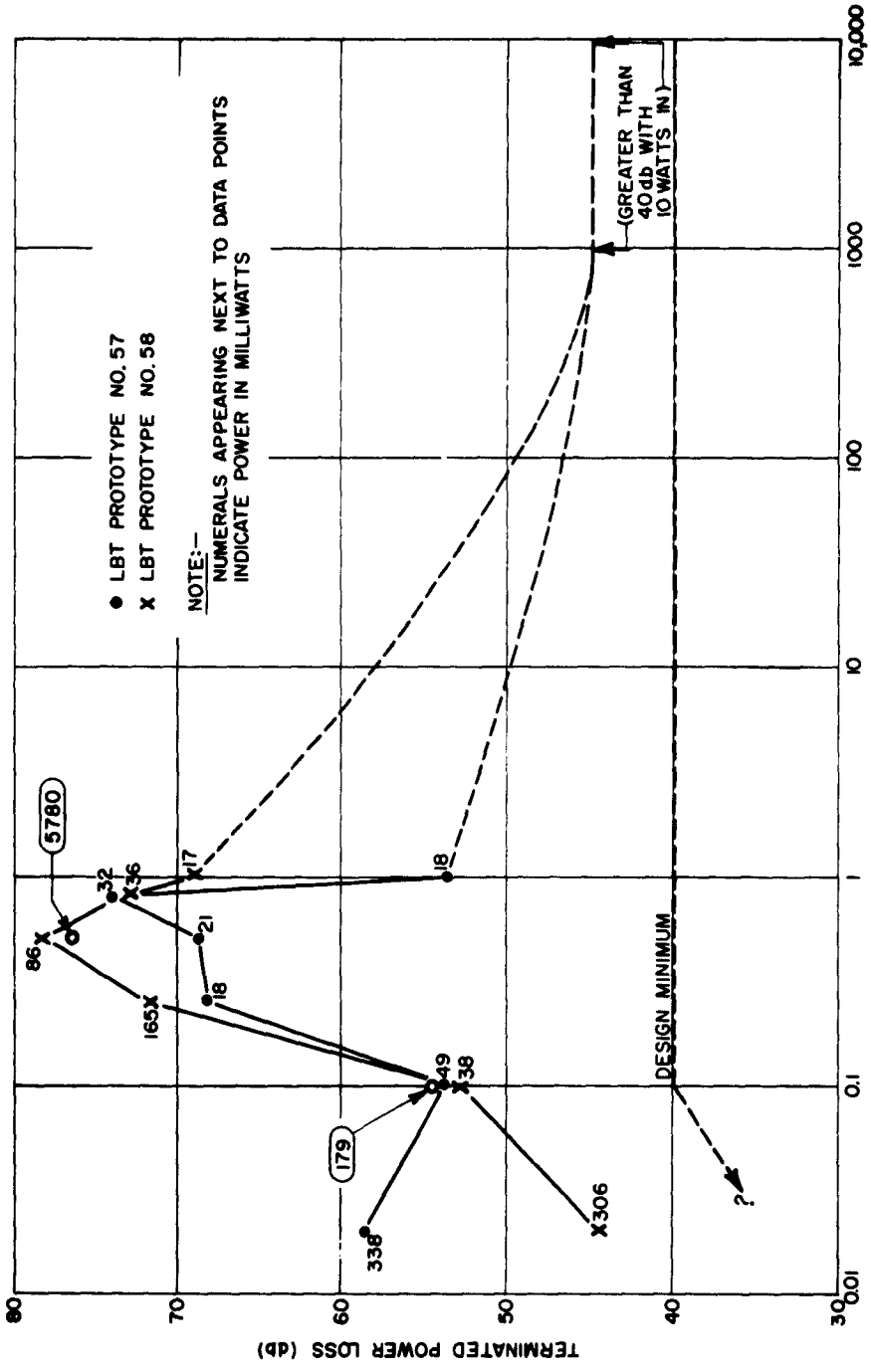

FIG. 1-2. TERMINATED (1Ω) POWER LOSS OF LBT PROTOTYPES

loss in excess of 40 db. Moreover, it was stated by Weston that their units would provide higher loss with higher power excitation. (This is somewhat born out by the two sets of data points plotted for XFMR No. 57 at 100 and 500 Kc). Because of the stated urgency, these data were presumed to be satisfactory in showing the nature of the frequency-loss characteristic, which, within the range of test frequencies, shows both units to exceed the loss specification.

At 1000 and 10,000 Mc it was not possible to detect an output signal above the equipment noise level. Since a signal of one milliwatt could have been readily detected, if it were present, and since the power input was on the order of 10 watts we conclude that the power loss is in excess of 40 db. For both frequencies, the 10 watts input power was delivered to a matched system comprising the one-ohm-loaded transformer preceeded by a matching section. Since the SWR determined at 1000 Mc was on the order of 10 to 1, experience tells us that a tuner used with this load should have insignificant loss.

Temperature rise was determined at both 1000 and 10,000 Mc for both units. Results of these tests are shown in Figure 1-3. In the interest of expediency these data were taken only for a 30-minute exposure. Weston had claimed that the temperature would reach stability within 40-minutes. Our first set of data (#58A @ 1000 Mc) indicated a very close approach to stability at 30-minutes, fostering the decision to terminate measurements after this lapse of time. Extrapolating the curves so as to predict maximum temperature at 40 minutes gives no cause for alarm. We are advised that the units should withstand 110°C temperature rise.

On the basis of the data collected so far, it would appear that model #58A has a slight edge, though either unit would satisfy requirements. This unit has the lowest temperature rise, and shows a better loss characteristic. In this regard, a word of warning is in order. Item #57 gives evidence of a loss characteristic which decreases

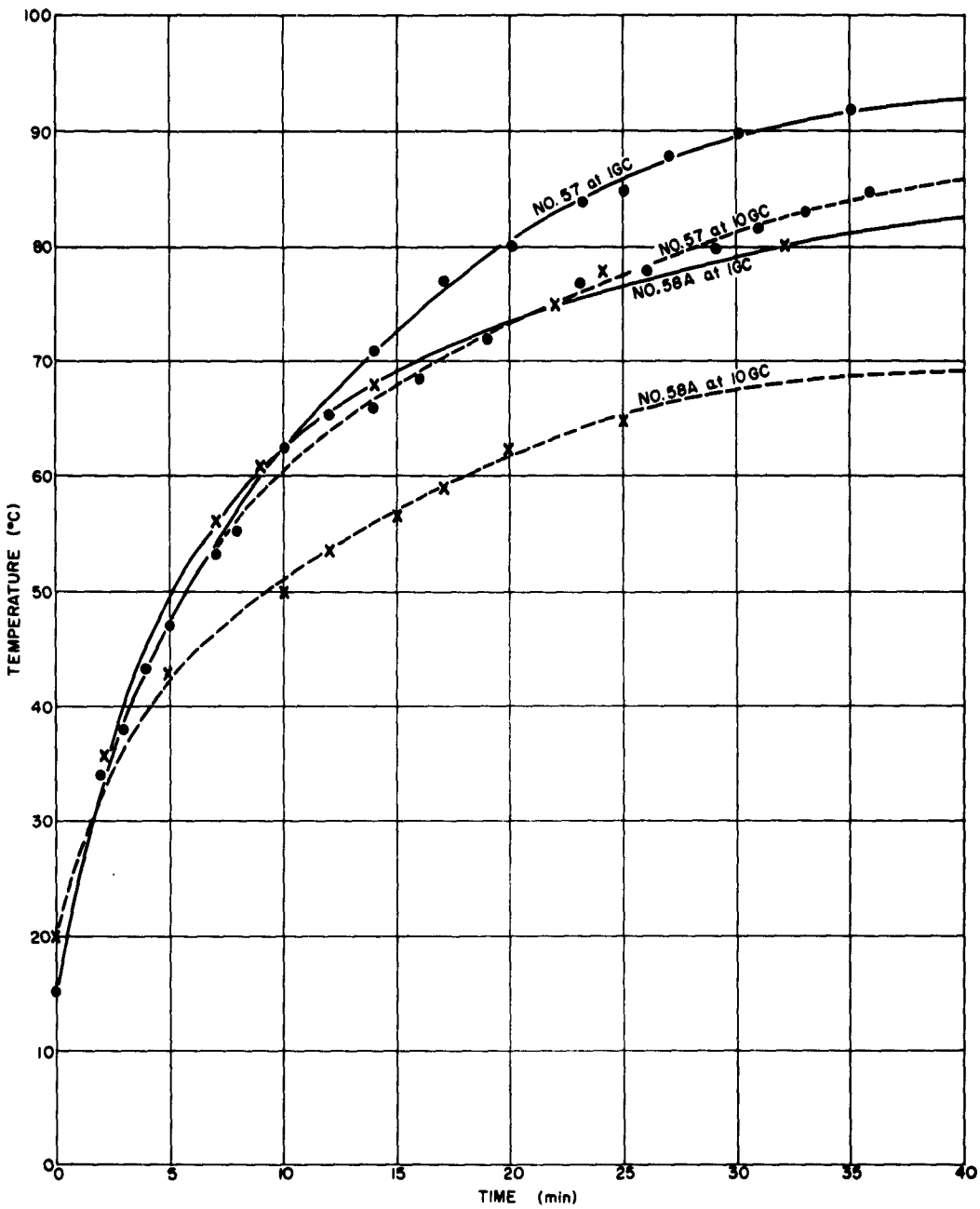

FIG. 1-3. TEMPERATURE RISE OF LBT PROTOTYPES
(10 watts input)

sharply at 1 Mc. This may indicate that the 40 db limit may be violated at a slightly higher frequency. An attempt was made to obtain data at 3 Mc to check this point, but frequency response of oscilloscope pre-amplifiers prohibited our acquiring meaningful data. Improved equipment will be assembled at another time to check this one point in question.

2. CALCULATIONS OF VOLTAGE MAXIMUMS AND MINIMUMS ON LOW LOSS TRANSMISSION LINES HAVING HIGH VSWR

Results of experiments of voltage maxima and minima from which we determine net power by the voltage min-max technique indicated that what was supposedly very low loss line was, in fact, absorbing considerable power. In order to resolve the difference, an analysis was performed.

Since the $\alpha\ \lambda$ product of the transmission line in question was not accurately known, a value of 0.00173 was deducted from manufacturer's literature, we decided to include in our investigation $\alpha\ \lambda$ products varying from 0.000346 to 0.0346. Two values for reflection coefficient were considered. The first was 49/51, corresponding to the case of a one-ohm resistive load terminating a 50 ohm system; the second was 39/41, a value determined from voltage min-max measurements.

The influence of voltage reflections from improper terminations upon power loss on transmission line systems is well covered in the literature.[1] We will use in our development the same notation as in Moore, as shown in Figure 2-1.

The total voltage on the uniform line of characteristic impedance Z_o and propagation constant $\Gamma = \alpha + j\ \beta$ can be expressed as

(1)Richard K. Moore, Traveling Wave Engineering, McGraw Hill, N.Y. 1960, pp. 155-183.

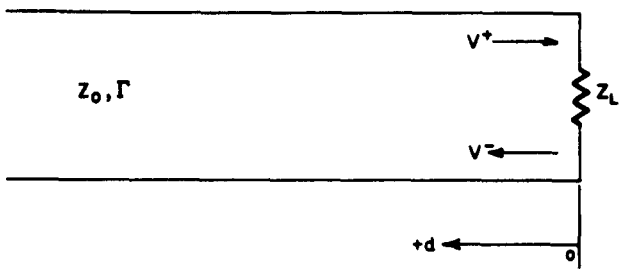

FIG. 2-1 TERMINATED UNIFORM TRANSMISSION LINE

$$\bar{V}_t = \bar{V}^+\left(e^{\Gamma d} + \bar{\rho}_o\, e^{-\Gamma d} \right) \qquad [1]$$

where d is the position coordinate

$\bar{V}^+$ is the voltage incident on the load

$\bar{\rho}_o$ is the reflection coefficient $= \left|\bar{\rho}_o\right| \angle\theta =$

$$\frac{Z_L - Z_o}{Z_L + Z_o} \text{ by definition}$$

$\bar{V}_t$ is the total voltage at a distance d from the load

$\beta = \frac{2\pi}{\lambda}$, the phase constant

α = the attenuation constant

λ = free space wavelength

The location of the maxima and minima of the total voltage can be found by setting the partial derivative of the magnitude of the bracketed quantity in equation 1 equal to zero. The resulting transcendental equation that defines these locations is

$$\alpha\left(e^{2\alpha d} - |\rho_o|^2 e^{-2\alpha d}\right) = 2\beta\,|\bar{\rho}_o|\,(\sin[2\beta d - \theta]) \qquad [2]$$

If we limit ourselves to systems in which $\alpha\lambda \leq .04$ and $|\rho_o| \cong 1$ equation 2 can be reduced to

$$e^{.08\frac{d}{\lambda}} - e^{-.08\frac{d}{\lambda}} = 100\pi\left(\sin\left[4\pi\frac{d}{\lambda} - \theta\right]\right) \qquad [3]$$

Further, if we are interested only in locations out to about $d = 2\lambda$, we can rewrite equations 3 at this worst location as

$$1.16 - \frac{1}{1.16} = 100\pi\left(\sin\ 4\pi\frac{d}{\lambda} - \theta\right) \qquad [4]$$

since $e^x \cong 1 + x$ for small x.

Within the limits imposed by our assumptions we may say that the locations of minima and maxima are given approximately by the solutions of

$$\frac{.3}{100\pi} \cong .001 = \sin\left[4\pi\frac{d}{\lambda} - \theta\right] \qquad [5]$$

The obvious approximate solutions ($.001 \cong 0$), those assumed in perfectly conducting line, are:

$$d = n\frac{\lambda}{4} + \frac{\theta}{\pi}\,\frac{\lambda}{4} \qquad [6]$$

The actual solutions to equation 5 determined by solving $\sin x = .001$, (in terms of $2\pi\frac{d}{\lambda}$) differ from equation 6, by less than .07 degree. Since there is so little difference between actual and approximate solutions we have used $\frac{\lambda}{4}$ as the distance between successive voltage extremes.

Using this approximation and assuming the termination to be a pure resistance of magnitude less than the characteristic impedance of the line (i.e. $\theta = 180°$) the maxima and minima can be written from equation 1 as

$$\bar{V}_{max} = \bar{V} + \left[e^{q \frac{\alpha}{2} \frac{\lambda}{2}} + \left|\bar{\rho}_o\right| e^{-q \frac{\alpha}{2} \frac{\lambda}{2}} \right] = \bar{V}_q \qquad [7]$$

$$q = 1, 3, 5, 7 - - - -$$

$$\bar{V}_{min} = \bar{V} + \left[e^{\eta \alpha \frac{\lambda}{2}} - \left|\bar{\rho}_o\right| e^{-\eta \alpha \frac{\lambda}{2}} \right] = \bar{V}_\eta \qquad [8]$$

$$\eta = 0, 1, 2, 3 - - - -$$

Under these conditions the minimums will occur at successive half wavelengths starting at the load and maximums at the intervening quarter-wavelength positions.

Equations 7 and 8 were evaluated for six values of $\alpha \lambda$ and two values of reflection coefficient. From these calculations, three significant parameters were determined:

V_n, the voltage minimum

$\frac{V_n - V_{n-1}}{V_{n-1}}$, the relative change in voltage maximum

$\frac{V_q - V_{q-1}}{V_{q-1}}$, the relative change in voltage maximum

These parameters are shown graphically in Figures 2-2 through 2-4. The actual calculations were carried to six significant figures, using the exponential expansion

$$e^x = 1 + x + \frac{x^2}{2!} + \frac{x^3}{3!} \text{ - - - -}$$

A useful fact uncovered in the setup of the calculations was that the approximation $e^x = 1 + x$ is accurate to

.01	if $x < .1414$
.001	if $x < .0447$
.0001	if $x < .01414$
.00001	if $x < .00447$
.000001	if $x < .001414$

Figure 2-3, indicates that the determination of the attenuation of a low-loss line is theoretically possible if the reflection coefficient is known and accurate voltage measurements can be made at the null positions of the voltage standing wave. Conversely, it is also theoretically possible to determine the reflection coefficient (real) if the null voltages and attenuation are known. These observations are of course subject to the approximations we made earlier, that the magnitude of the reflection coefficient is close to unity and the $\alpha\ \lambda$ product is within the range investigated.

These results validate a number of seemingly questionable observations made in experiments to verify the voltage min-max power measurement technique. First, as indicated by Figure 2-4, we should expect the voltage maximum changes along the line to be insignificantly small; any change observed should give cause to suspect the measuring equipment calibration. On the other hand, according to the evidence of Figure 2-3, we can expect voltage minima to change drastically along

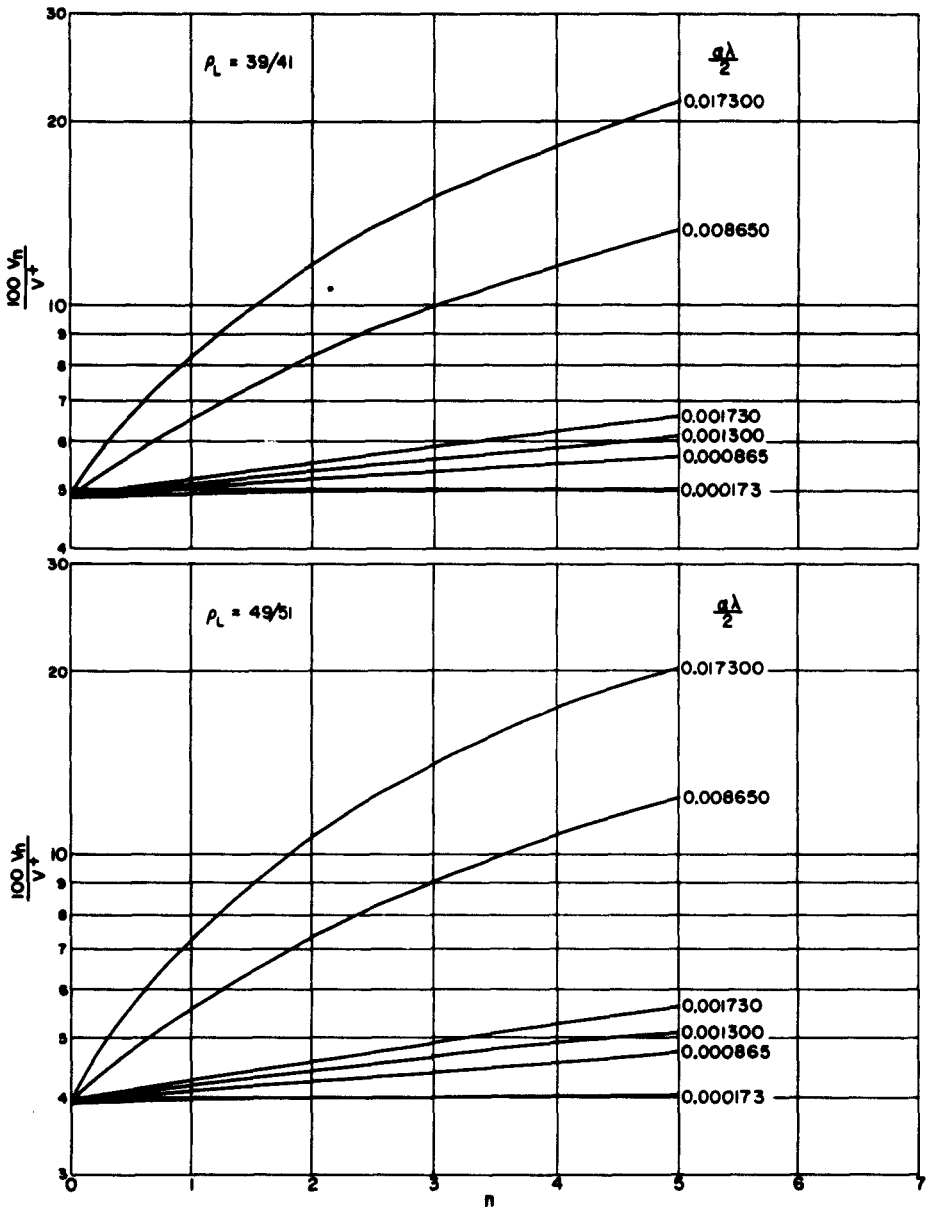

FIG. 2-2. RELATIVE MAGNITUDE OF V_{min} ALONG LOW LOSS TRANSMISSION LINE

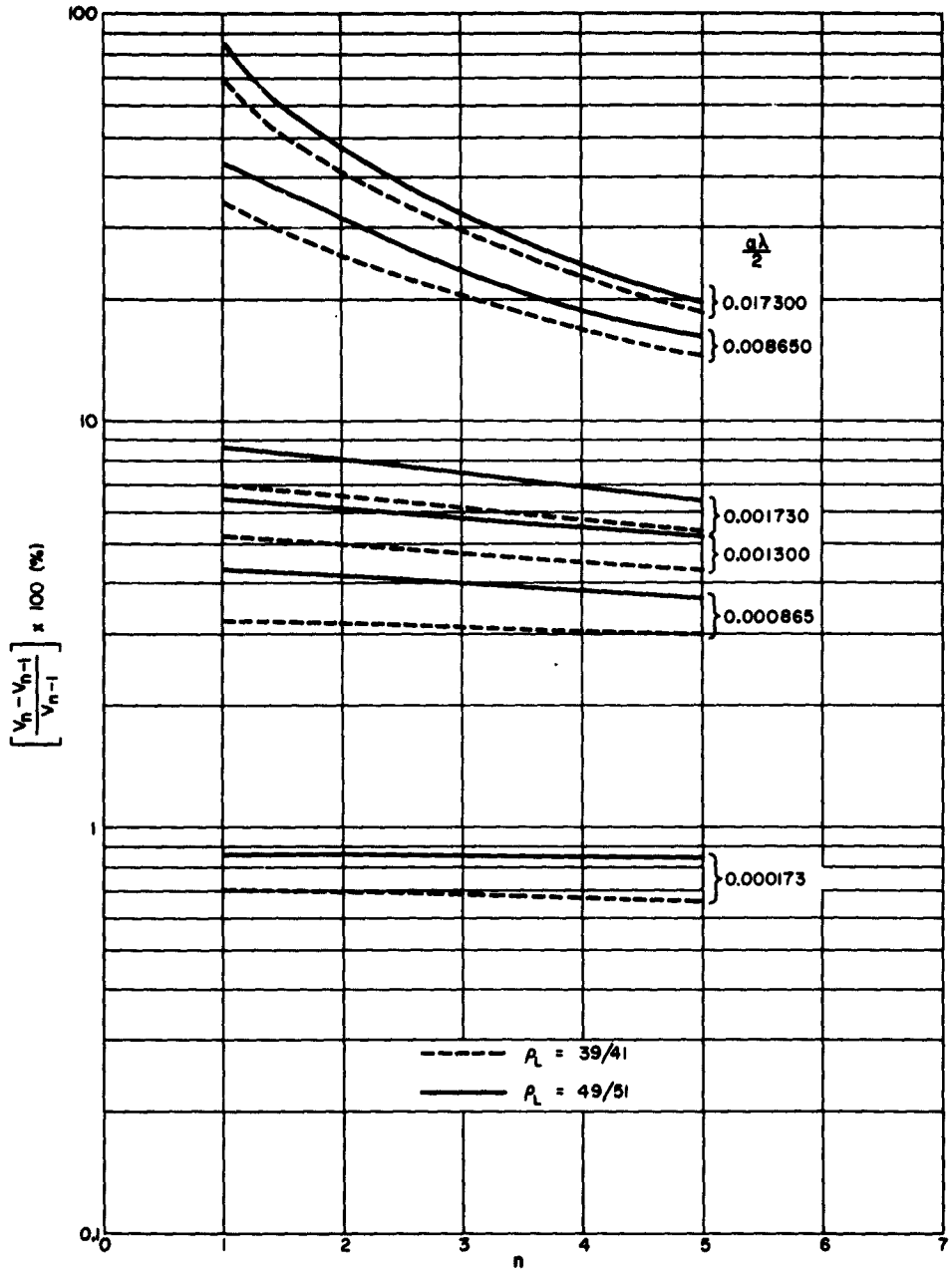

FIG. 2-3. CHANGE IN V_{min} ALONG LOW LOSS TRANSMISSION LINE

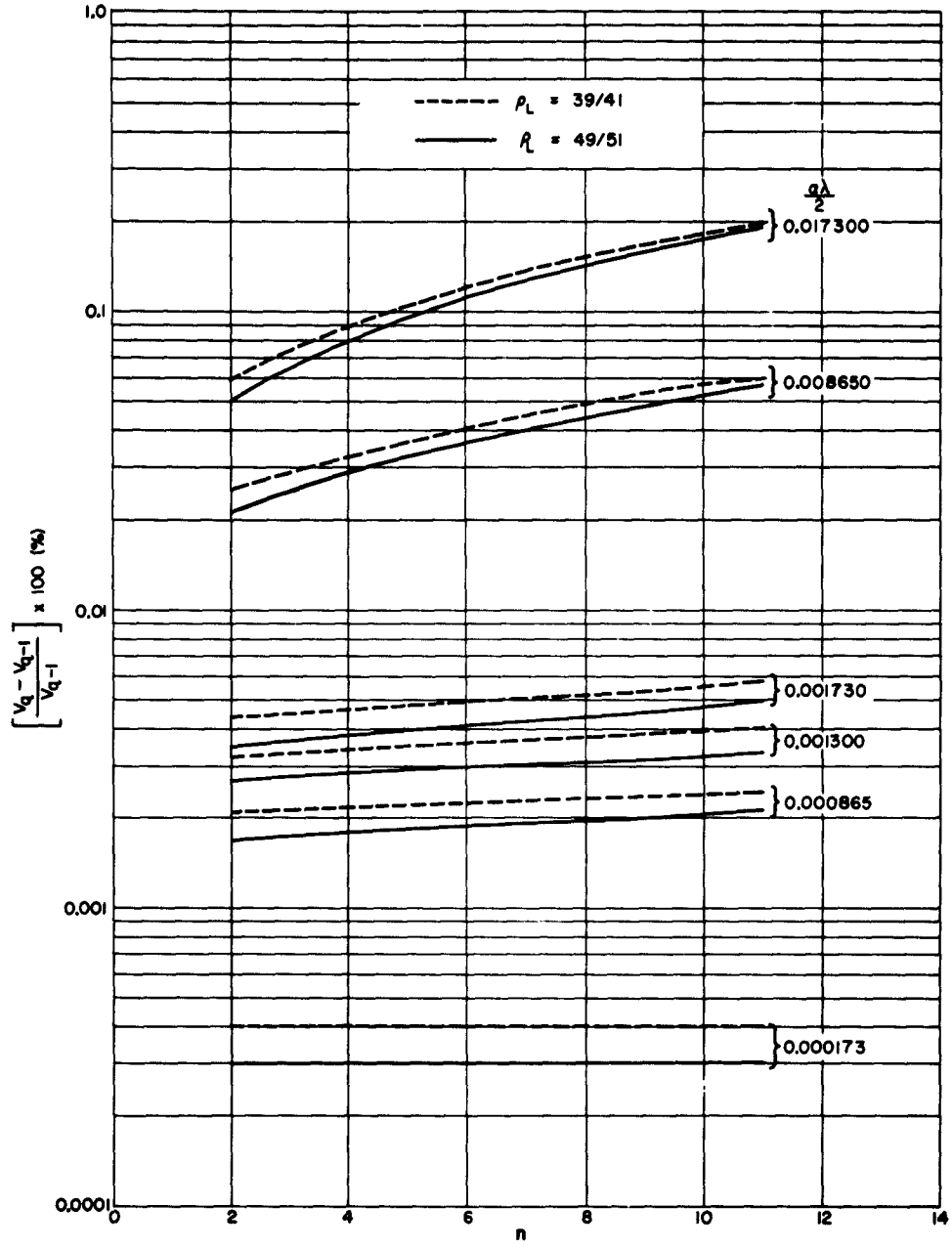

FIG. 2-4. CHANGE IN V_{max} ALONG LOW LOSS TRANSMISSION LINE

the line. The values predicted by these analyses are in good agreement with experimental data presented in the preceding report. An auxiliary consequence of comparing results of these analyses with experimental data is the verification of the manufacturer's value for the $\alpha\lambda$ product for the line used in experimental work.

3. PRELIMINARY VOLTAGE MIN-MAX POWER DETERMINATIONS IN WAVEGUIDE

To evaluate the RF power delivered to an electroexplosive device we have developed an RF power transmission system which is terminated by an impedance matching network and a mount containing the device. Adjustment of the matching network transforms the impedance of the device to that of the transmission line. If the network is lossless, the incident power into the network equals the power dissipated in the device. We have found, however, that losses in all transmission line components located between the power source and the device increase as a function of the standing wave ratio at the termination. To determine the losses, or rather the system efficiency, with a specific device in the terminating position, we must measure the net power delivered to the base of the device, and at the same time measure the power delivered to the matched system. Of the several methods that we have investigated for making net power measurements we have found the voltage min-max method to be the most promising, considering both ease and accuracy. A method for calibrating a slotted transmission line to make this measurement and a description of the application of this method for determing firing system efficiency are discussed here. This technique has been demonstrated to be feasible for coaxial systems; in the following discussion we have made the needed adaptation to waveguide systems. Evaluation of the protected MARK 7 MOD 0 ignition element at a frequency above 1000 Mc will require this sort of system.

3.1 Slotted Line Probe Calibration Development

The net power through an arbitrarily terminated transmission line can be expressed in terms of the voltage standing wave maximum and minimum[1] by

$$P_n = \frac{V_{max} V_{min}}{R_o} \quad \text{(watt)} \qquad [1]$$

where P_n = net power (watt)

V_{max} = RMS magnitude of line voltage at a voltage maximum (volt)

V_{min} = RMS magnitude of line voltage at a voltage minimum (volt)

R_o = characteristic impedance of transmission line (ohm)

A slotted section of transmission line is used to measure V_{max} and V_{min}. To do this, a relationship must be established between the slotted line probe output voltage and the true RF voltage on the transmission line. By terminating the line with a power meter whose input impedance equals R_o, Fig. 3-1, we reduce the standing wave ratio to unity so that the line voltage at any position V_x is related to the load power P_L by

$$P_L = \frac{V_x^2}{R_o} \quad \text{(watt)} \qquad [2]$$

Instead of finding V_x directly, we shall simplify our work if we determine D_x, the probe output given by

---

1 Handbook of Electrical Measurements; Edited by Moe Wind, Polytechnic Institute of Brooklyn, July 1956.

$$\frac{V_x^2}{R_o} = f(D_x) \quad \text{(watt)} \qquad [3]$$

In an arbitrarily terminated system, values of D_x, (D_{max} and D_{min}), are obtained from the slotted line as shown in Fig. 3-2. These are related to the corresponding quantities V_{max} and V_{min} by equation [3] which may be rewritten

$$V_{max} = \sqrt{f(D_{max})\, R_o} \quad \text{(volt)} \qquad [4]$$

$$V_{min} = \sqrt{f(D_{min})\, R_o} \quad \text{(volt)} \qquad [5]$$

Combining [4] and [5] with [1] we get

$$P_n = \left[f(D_{max})\ f(D_{min})\right]^{\frac{1}{2}} \quad \text{(watt)} \qquad [6]$$

If the calibration curve is used only in the linear range (a result of the square law response of crystal detectors when the input power is small), then $f(D_x) = kD_x$, and the calibration constant k is obtained from

$$k = \frac{V_x^2\, R_o}{D} = \frac{P_L}{D} \quad \text{(watt/volt)} \qquad [7]$$

Equation [6], may then be reduced to

$$P_n = k\left[D_{max}\, D_{min}\right]^{\frac{1}{2}} \quad \text{(watt)} \qquad [8]$$

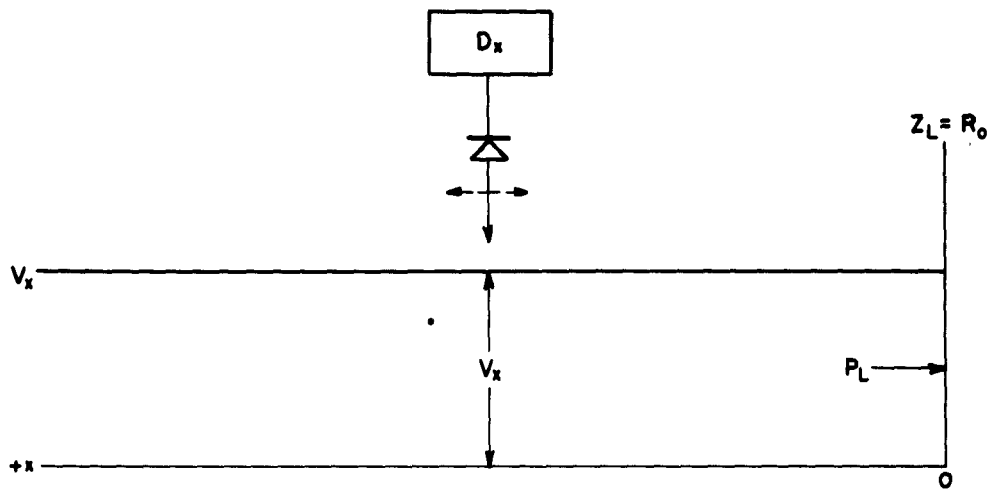

FIG. 3-1. PROBE CALIBRATION

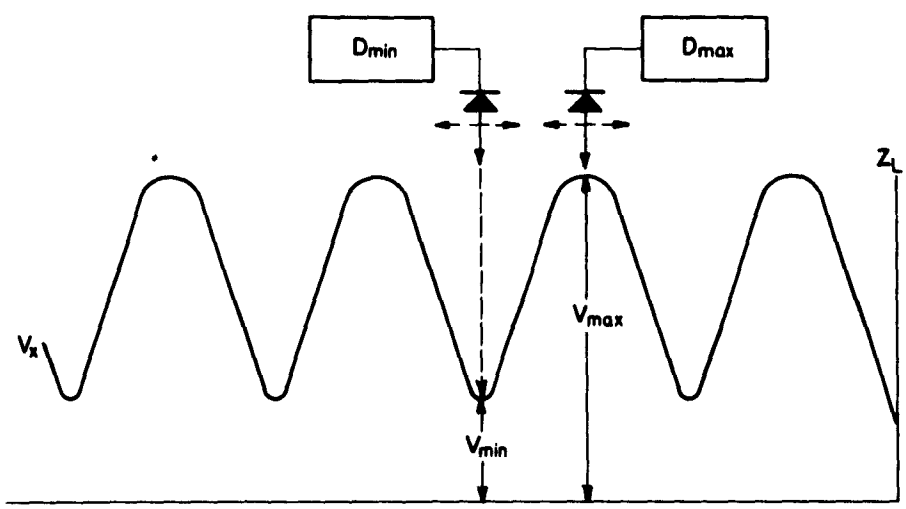

FIG. 3-2. CALIBRATION PROBE V_{max} AND V_{min} MEASUREMENTS

The elimination of R_o from the final equation is essential if we are to use this approach for measuring net power in waveguide systems.

The slotted line calibration can also be used to determine the standing wave ratio (S) at the termination. From equations [4] and [5] we may develop the formula

$$S = \frac{V_{max}}{V_{min}} = \sqrt{\frac{f(D_{max})\, R_o}{f(D_{min})\, R_o}} \qquad [9]$$

For measurements within the square-law region of the detector this reduces to

$$S = \sqrt{\frac{D_{max}}{D_{min}}} \qquad [10]$$

3.2 System Efficiency Measurement at 10 Gc

The voltage min-max power measuring technique was applied to a 10 Gc waveguide firing system to determine its efficiency for a specific electroexplosive device. This work was done in conjunction with another program since the same procedures will be used in testing the protected MARK 7 MOD 0.

There are three phases involved in a precision firing test, a test which requires a system efficiency calibration. First, the slotted line probe is calibrated. Second, with the device to be tested terminating the line, the system efficiency is determined. Third, the firing test is performed with the transmission line system exactly as it was in the efficiency test.

3.2.1 Slotted Line Probe Calibration

Figure 3-3 is a block diagram of the system for calibrating the slotted line probe. A low-level power source is used during the first two phases of the calibration, since we want the system efficiency to be based on the "cold" impedance of the electroexplosive device. The klystron which is used has the property of producing an output which is sharply tuned to a specific frequency which is necessary if we are to obtain a sharply defined V_{min} on the standing wave. Although the probe used with the slotted line is supposedly broadband, we do not permit any variation of frequency during the efficiency calibration since it might change the coupling factor between the probe and the line. A directional coupler and frequency meter are used to monitor the frequency.

The slide-screw tuner located between the slotted line and the thermistor is used to match the thermistor mount to the transmission line so that the line voltage is flat. This is done by tuning the slide-screw tuner for a maximum transfer of power to the RF power meter. If the match is good, the standing wave ratio on the slotted line will be almost unity. Any slight deviations can be averaged out by setting the position of the slotted line probe equidistant between a maximum and a minimum. Since the slide-screw tuner is used to "match out" standing waves which are already close to unity the loss with it can be assumed negligible.

The depth to which the probe penetrates the line is very important. The probe appears as a shunt admittance across the line and if it penetrates too deeply it will load the line sufficiently to cause measurement error. A check for too much coupling can be made by watching the power meter while traversing the line with the probe. If the penetration is too deep, the reading of the power meter terminating the line will change as the probe couples more or less power from the line depending on its location relative to the voltage standing wave. This effect is accentuated if the power meter is not matched to the line. Through

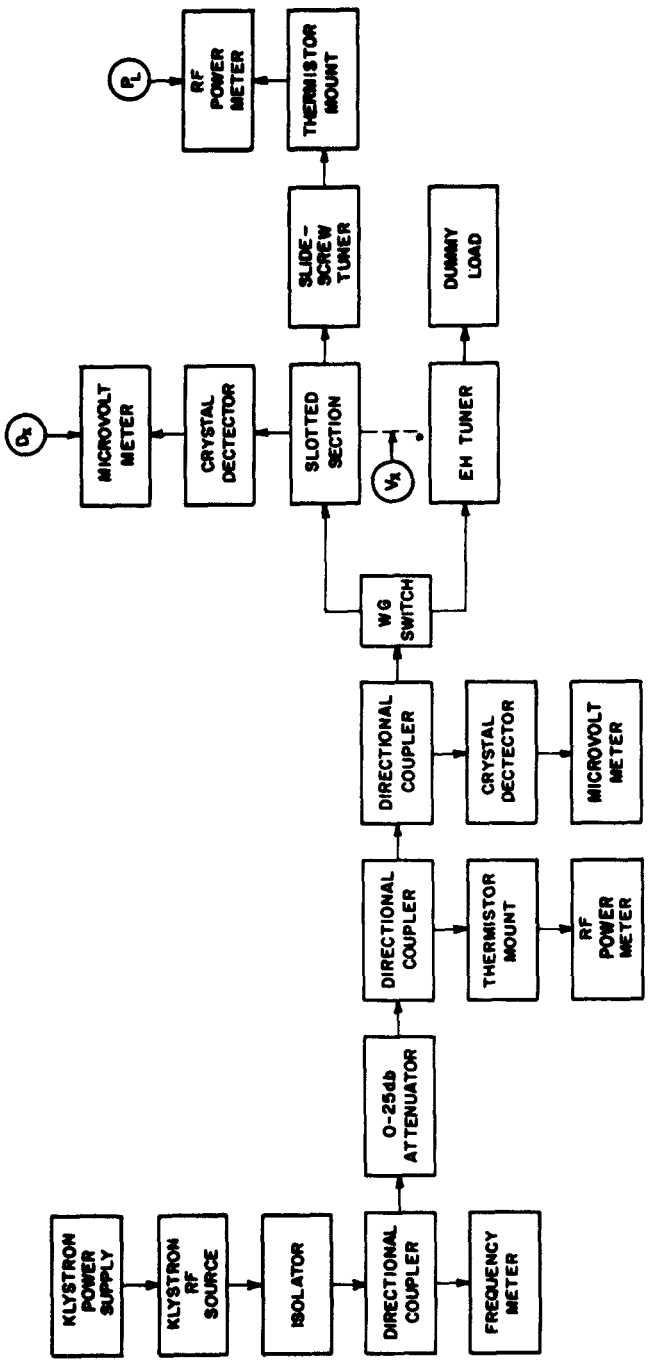

FIG. 3-3. PROBE CALIBRATION SYSTEM

experimentation we have established a probe penetration as that which produces about 30 mv of probe output voltage to every 10 mw of RF power. This coupling factor, while sufficient to drive the microvoltmeter attached to the probe, is small enough that there is negligible loading of the transmission line. A calibration curve of D vs P_L is plotted on log-log paper so as to expand the lower part of the curve. We found that for probe output voltages of less than about 30 mv the detector benaved as a square-law device, with the output voltage D proportional to line power P_L. Figure 3-4 shows the 45-degree calibration curve. Because of the noise in low-level RF power meter readings we are unable to plot accurately any points below 0.3 mv. We can say, however, that the device behaves as a square-law detector over approximately 30 db of dynamic range which (from Equation 9) is equivalent to standing wave ratios of about 30:1. If we are to measure ratios higher than this we must extend the calibration curve beyond the square-law region using a calorimetric power meter as shown in Figure 3-4.

3.2.2 System Efficiency Determination

Figure 3-5 illustrates a block diagram of the firing system when making a system efficiency measurement. An unaltered (live) electro-explosive device of the type being tested is mounted as if for actual firing. With the applied frequency the same as for the calibration, and the incident power level small (about 1 mw), the E-H tuner is adjusted for a null at the reflected power indicator. This null should represent a reflected power of less than 3% of the incident power. The slotted line probe is then positioned at a voltage maximum. Because of the knowledge obtained from calibrating the probe, we set the klystron output so that D_{max} is about 30 mv, the upper limit of the square-law response. Then the probe is accurately positioned at a voltage minimum. At this point, the RF power is turned off so that the microvoltmeter and the power meter connected to the incident power directional coupler can be

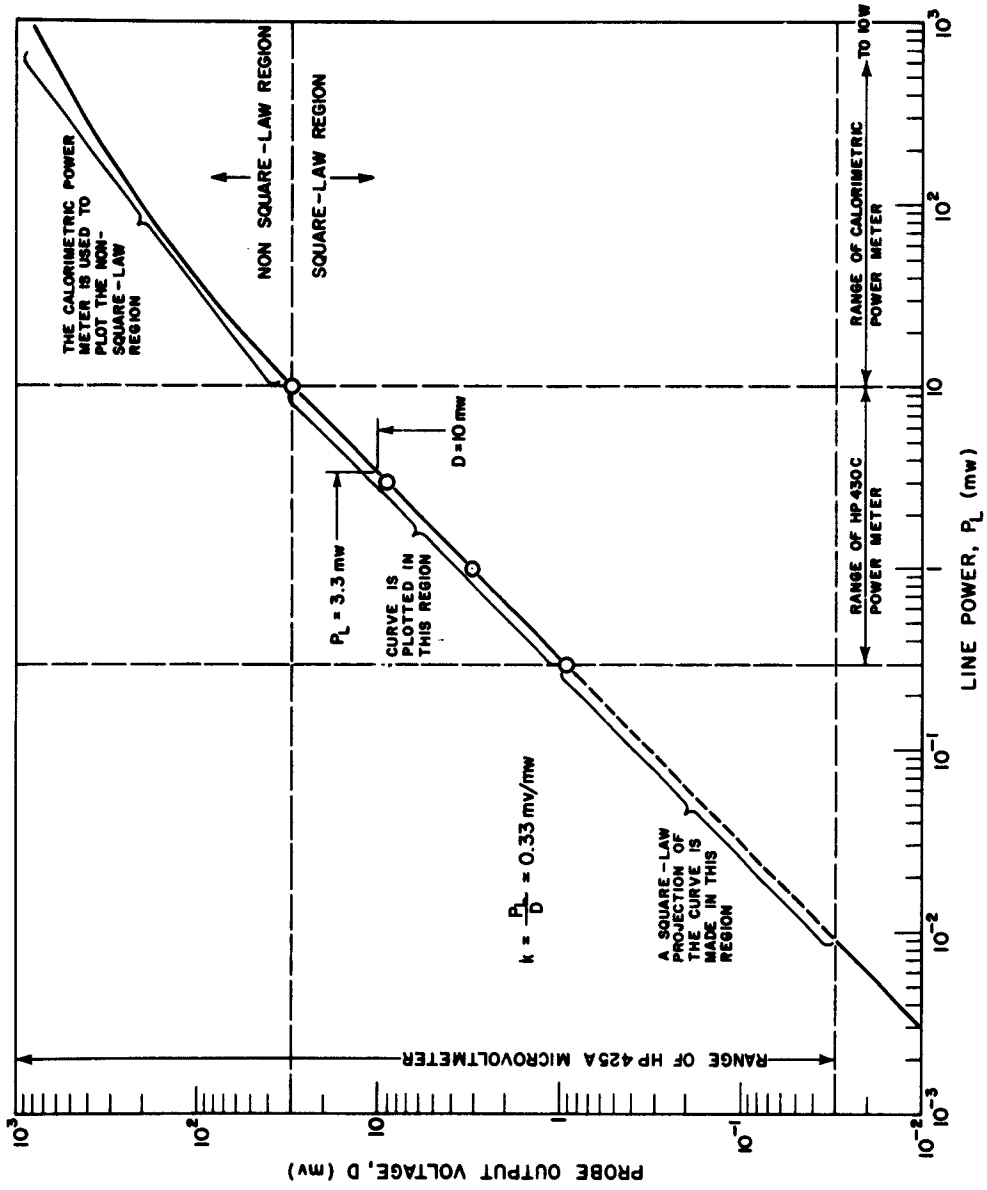

FIG. 3-4. VOLTAGE PROBE CALIBRATION

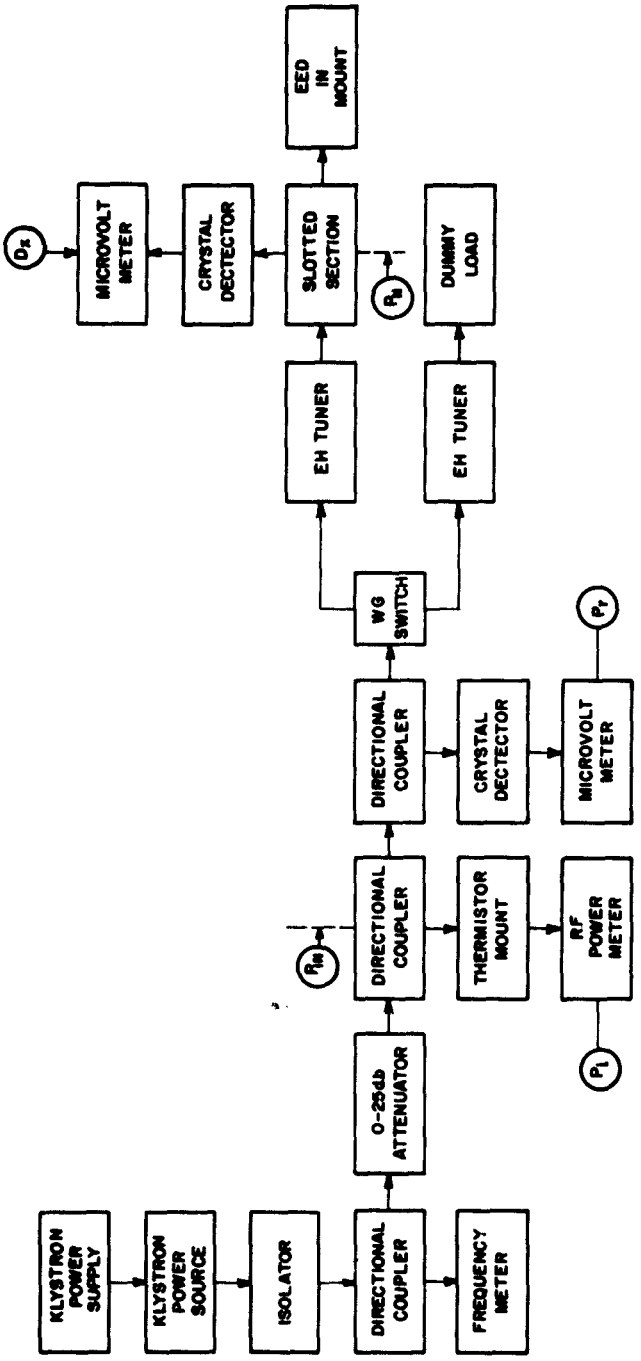

FIG. 3-5. SYSTEM FOR DETERMINING EFFICIENCY

accurately zeroed. When the system is turned on the incident power, p_i, and probe indication, D_{min}, are determined. The probe is moved to a maximum where D_{max} is read. The net power through the slotted section is determined from equation [8], repeated here for convenience.

$$P_n = k \left(D_{max}\, D_{min}\right)^{\frac{1}{2}} \quad \text{(watt)} \qquad [8]$$

The system efficiency calibration factor C, which includes losses in the slotted line, E-H tuner and directional coupler, and the directional couplers' coupling factor is found from

$$C = \frac{P_n}{p_i} \qquad [11]$$

This means that the net power to this specific electroexplosive device is related to the power measured prior to the matching network by

$$P_n = C\, p_i \qquad [12]$$

3.2.3 Firing Test Precautions

The RF firing test is performed with the slotted section in place since it was included in the system calibration. The calibrated probe, however, must be removed since the RF energy required for firing may be large enough to damage the detector. An insensitive probe inserted in its place is lightly coupled to the line and supplies a "start" voltage to the chronograph at the beginning of a test. The high power RF generator used for the firing test should operate at approximately the same frequency as that used for the calibration.

3.3 Proposed System Developments

Several system limitations were discovered while making the 10 Gc system calibration. If we desire to operate the slotted line probe detector within its square-law region we are limited to about 30 db of dynamic range, the result of a lack of a dc microvoltmeter sensitive enough to read voltages lower than 10 microvolts on the one hand and a maximum square-law output from the crystal of about 30 mv on the other.

This limits our standing wave measurements to values of less than about 30 to 1. Noise signals present in the microvoltmeter reading when attempting to measure minimum line voltages of about 30 microvolts further limit the accuracy of the net power measurement.

To provide a more accurate means of measuring high standing wave ratios on waveguide slotted sections we are designing an adjustable probe whose penetration is set by a micrometer screw.

The probe detectors will be connected to a meter having a full scale deflection within the square-law limit of the probe. With the slotted section connected to the power meter as described in Section 3.2.1 of this report we shall make a calibration of probe depth corresponding to RF voltage on the line, to give a constant full scale reading of the probe detector meter. If this calibration proves to be straightforward we should be able to measure standing wave ratios by varying the probe depth for measurements of V_{max} and V_{min}. In this way we hope to eliminate the need for a very sensitive microvoltmeter, the requirement that the probe detector operate as a square-law device over a wide range of power, and inconvenience resulting from the non-uniform loading of the transmission line, when making V_{max} and V_{min} measurements.

ACKNOWLEDGEMENTS

John P. Warren contributed in large measure to the experimental results given in Section 1. For the development of Section 2, the work of Ramie H. Thompson is gratefully acknowledged. Recognition is given George McKay for the work reported in Section 3.

Paul F. Mohrbach
Group Leader

Norman P. Faunce
Project Leader

Approved by:

E. E. Hannum, Manager
Applied Physics Laboratory

Francis L. Jackson
Director of Laboratories

P-B1980-6

DISTRIBUTION LIST

U.S. Naval Weapons Laboratory
Dahlgren, Virginia
Attn: Code: WHR (2)

Chief, Naval Operations (OP-411H)
Department of the Navy
Washington 25, D.C.

Chief, Bureau of Naval Weapons
Department of the Navy
Washington 25, D.C.
Code: C-132
RAAV-3421
RM-15
RMMO-224
RMMO-235
RMMO-32
RMMO-33
RMMO-4
RMMO-43
RMMO-44
RMMP-343
RREN-32
DIS-313 (4)

Chief, Bureau of Yards and Docks
Department of the Navy
Washington 25, D.C.
Attn: Code: D-200

Commander
U.S. Naval Ordnance Laboratory
White Oak, Md.
Code: ED
NO
LV
Technical Library

Commanding Officer
U.S. Naval Ordnance Laboratory
Corona, California
Attn: Code 561

Commander
U.S. Naval Ordnance Test Station
China Lake, California
Code: 556
4572

Commanding Officer
U.S. Naval Air Development Center
Johnsville, Penna.
Code: EL 94

Officer-in-Charge
U.S. Naval Explosive Ordnance Disposal
Technical Center
U.S. Naval Propellant Plant
Indian Head, Md.

Commanding Officer
U.S. Naval Underwater Ordnance Station
Newport, R.I.

Director
U.S. Naval Research Laboratory
Washington 25, D.C.
Code: 5410 (2)

Commandant of the Marine Corps
Washington 25, D.C.
Code: AO4C

Commander
Pacific Missile Range
P.O. Box 8
Point Mugu, California
Attn: Code 3260

Commanding Officer and Director
U.S. Navy Electronics Laboratory
San Diego 52, California
Attn: Library

Commanding Officer
U.S. Naval Ammunition Depot
Crane, Indiana
Code 34

DISTRIBUTION LIST (Cont.)

Commanding Officer
U.S. Naval Ordnance Plant
Macon, Georgia
Attn: Code PD 270

Commander Naval Air Force
U.S. Atlantic Fleet (CNAL 724B)
U.S. Naval Air Station
Norfolk 11, Va.

Commander Training Command
U.S. Pacific Fleet
c/o U.S. Fleet Anti-Submarine Warfare School
San Diego 47, California

Commanding General
Headquarters, Fleet Marine Force, Pacific
c/o Fleet Post Office
San Francisco, California
Attn: Force Communications Electronic Officer

Commander-in-Chief
U.S. Pacific Fleet
c/o Fleet Post Office
San Francisco, California
Attn: Code 4

Commander Seventh Fleet
c/o Fleet Post Office
San Francisco, California

Commander
New York Naval Shipyard
Weapons Division
Naval Base
Brooklyn 1, New York
Attn: Code 290

Commander
Pearl Harbor Naval Shipyard
Navy No. 128, Fleet Post Office
San Francisco, California
Attn: Code 280

Commander
Portsmouth Naval Shipyard
Portsmouth, New Hampshire

Department of the Army
Office Chief of Ordnance
Washington 25, D.C.
Attn: ORDGU-SA
ORDTN
ORDTB (Research & Special Projects)

Office Chief Signal Officer
Research & Development Division
Washington 25, D.C.
Attn: SIGRD-8

Commanding Officer
Diamond Ordnance Fuze Laboratories
Washington 25, D.C.
Attn: Mr. T.B. Godfrey

U.S. Army Nuclear Weapon Coordination Group
Fort Belvoir, Virginia

Director
U.S. Army Engineer Research & Development Labs.
Fort Belvoir, Va.
Attn: Chief, Basic Research Group

Commanding Officer
Picatinny Arsenal
Dover, New Jersey
Attn: Artillery Ammunition & Rocket Development Lab. Mr. S.M. Adelman
Attn: Evaluation Unit, Instrumentation Section, Bldg. 352 Mr. A. Grinoch

Commanding General
Headquarters 2DRAADCOM
Oklahoma City, AFS
Oklahoma City, Oklahoma

DISTRIBUTION LIST (Cont.)

Commanding Officer
U.S. Army Signal Research &
Development Lab.
Fort Monmouth, N.J.
Attn: SIGEM/E1-GF

Commande
U.S. Army Ordnance
Frankford Arsenal
Phila. 37, Penna.

Commander
U.S. Army Rocket & Guided
Missile Agency
Redstone Arsenal, Alabama
Attn: ORDXR-R (Plans)

Commanding Officer
Office of Ordnance Research,
U.S. Army
Box CM, Duke Station
Durham, North Carolina
Attn: Internal Research Div.

Commanding General
White Sands Missile Range
New Mexico
Attn: ORDBS-G3

Commanding Officer
White Sands Missile Range,
New Mexico
U.S.A. SMSA
Attn: SIGWS-AJ

Commanding General
U.S. Army Electronic Proving
Ground
Ft. Huachuca, Arizona

Director of Office of Special
Weapons Developments
U.S. Continental Army Command
Ft. Bliss, Texas
Attn: Capt. C.I. Peterson
T S Control Officer

Headquarters
Air Research & Development Command
Andrews Air Force Base
Washington 25, D.C.
Attn: RDMMS-3

Commander
Air Force Missile Test Center
Patrick Air Force Base, Florida
Attn: Code MTRCF

Director Nuclear Safety
Kirtland AFB, N.M. Research
Attn: AFCNS

Headquarters
Ogden Air Material Area
Hill Air Force Base
Ogden, Utah
Code OOYSS

Commander
Air Force Missile Development
Center
Holloman Air Force Base
Alamagordo, New Mexico

Griffiss AF Base
RADC, New York
Attn: RCLS/Philip L. Sandler

Commander
Air Force Special Weapons Center
Kirtland Air Force Base
Albuquerque, New Mexico
Attn: SWVSA

DISTRIBUTION LIST (Cont.)

Director of Missile
Safety Research
Deputy IG for Safety
Norton AFB, California

Commanding General
Air Fleet Marine Force, Pacific
MCAS, El Toro
Santa Ana, California

Strategic Air Command
Offutt Air Force Base, Nebraska
Attn: DOSDM

Commander
Headquarters Ground Electronics
Engineering Installation Agency
Griffiss Air Force Base
Rome, New York
Code ROZMWT

Armed Services Explosives Safety Bd.
Department of Defense
Rm. 2075, Gravelly Point, Bldg. T-7
Washington 25, D.C.

Headquarters
Armed Services Technical Information
Agency (TIPCR)
Arlington Hall Station
Arlington 12, Virginia
VIA: U.S. Naval Weapons Lab.
Dahlgren, Virginia
Code WHR (10)

Commander
Field Command
Defense Atomic Support Agency
Albuquerque, New Mexico
Attn: FCDR3

U.S. Atomic Energy Commission
Division of Military Application
Washington 25, D.C.

Defense Research Staff
British Embassy
3100 Mass. Ave., N.W.
Washington 8, D.C.
Attn: Mr. G.R. Nice
VIA: U.S. Naval Weapons Lab.
Dahlgren, Va.
Code WHR

Naval Member
Canadian Joint Staff
2450 Mass. Ave., N.W.
Washington 8, D.C.
Attn: Staff Officer (Weapons)
VIA: U.S. Naval Weapons Lab.
Dahlgren, Va.
Code WHR

American Machine & Foundry Co.
Alexandria Division
1025 N. Royal St.
Alexandria, Va.

Atlas Powder Co.
Reynolds Ordnance Section
P.O. Box 271
Tamaqua, Penna.
Attn: Mr. R. McGirr

The Bendix Corp.
Scintilla Div.
Sidney, N.Y.
Attn: R.M. Purdy

Bermite Powder Co.
22116 W. Soledad Canyon Rd.
Saugus, California
Attn: Mr. L. Lo Fiego

Chance Vaught Corp.
P.O. Box 5907
Dallas, Texas, (22)
Attn: R.D. Henry

DISTRIBUTION LIST (Cont.)

Aerojet-General Corp.
P.O. Box 296
Azusa, California
Attn: Myra Z. Grenier, Librarian

Gruman Aircraft Engineering Corp.
Weapons Systems Dept.
Bethpage, L.I., N.Y.
Attn: Mr. E.J. Bonan

Hanscom Air Force Base, Mass.
Codes: AFCCDD/CCSEI-1
Attn: Capt. Long

Jansky & Bailey, Inc.
1339 Wisconsin Ave., N.W.
Washington, D.C.
Attn: Mr. F.T. Mitchell, Jr.
Contract N178-7604

Lockheed Aircraft Corp.
P.O. Box 504
Sunnyvale, California
Attn: Missile Systems Div. Dept. 62-20
Mr. I.B. Gluckman
Attn: Missiles and Space Div. Dept.
81-62, Mr. E.W. Tice
Attn: Missiles and Space Div. Dept.
81-71, Mr. R.A. Fuhrman

McCormick Selph Associates
Hollister, California
Attn: Technical Librarian

Midwest Research Institute
425 Volker Blvd.
Kansas City, Missouri
Attn: Security Officer

RCA Service Co.
Systems Engineering Facility
Government Service Dept.
838 N. Henry St.
Alexandria, Va.
Attn: Mr. C.M. Fisher

Sandia Corp. (Div. 1262)
Albuquerque, New Mexico
VIA: FCDASA

University of Denver
Denver Research Institute
Denver 10, Colorado
Attn: Mr. R.B. Feagin

U.S. Flare Div. Atlantic Res. Corp.
19701 W. Goodvale Rd.
Saugus, California
Attn: Mr. N.E. Eckert, Head
R & D Group

Vitro Laboratories
14000 Georgia Ave.
Silver Spring, Md.
Attn: Miss C.M. Jaques, Librarian

Welex Electronics Corp.
Solar Bldg. Suite 201
16th and K Sts., N.W.
Washington 5, D.C.

North American Aviation, Inc.
Communication Services
4300 E. 5th Ave.
Col. 16, Ohio